Journal of Structural Biology 174 (2011) 527–535

Contents lists available at ScienceDirect

Journal of Structural Biology

journal homepage: www.elsevier.com/locate/yjsbi

Bone mineralization proceeds through intracellular calcium phosphate loaded vesicles: A cryo-electron microscopy study

Julia Mahamid [a,*], Amnon Sharir [b,c], Dvir Gur [a], Elazar Zelzer [b], Lia Addadi [a], Steve Weiner [a]

[a] Department of Structural Biology, Weizmann Institute of Science, 76100 Rehovot, Israel
[b] Department of Molecular Genetics, Weizmann Institute of Science, 76100 Rehovot, Israel
[c] Koret School of Veterinary Medicine, The Robert H. Smith Faculty of Agriculture, Food and Environment, Hebrew University of Jerusalem, 76100 Rehovot, Israel

ARTICLE INFO

Article history:
Received 4 January 2011
Received in revised form 18 March 2011
Accepted 18 March 2011
Available online 2 April 2011

Keywords:
Biomineralization
Mouse model
Osteoblast
Calvaria
Carbonated hydroxyapatite
Transient precursor

ABSTRACT

Bone is the most widespread mineralized tissue in vertebrates and its formation is orchestrated by specialized cells – the osteoblasts. Crystalline carbonated hydroxyapatite, an inorganic calcium phosphate mineral, constitutes a substantial fraction of mature bone tissue. Yet key aspects of the mineral formation mechanism, transport pathways and deposition in the extracellular matrix remain unidentified. Using cryo-electron microscopy on native frozen-hydrated tissues we show that during mineralization of developing mouse calvaria and long bones, bone-lining cells concentrate membrane-bound mineral granules within intracellular vesicles. Elemental analysis and electron diffraction show that the intracellular mineral granules consist of disordered calcium phosphate, a highly metastable phase and a potential precursor of carbonated hydroxyapatite. The intracellular mineral contains considerably less calcium than expected for synthetic amorphous calcium phosphate, suggesting the presence of a cellular mechanism by which phosphate entities are first formed and thereafter gradually sequester calcium within the vesicles. We thus demonstrate that *in vivo* osteoblasts actively produce disordered mineral packets within intracellular vesicles for mineralization of the extracellular developing bone tissue. The use of a highly disordered precursor mineral phase that later crystallizes within an extracellular matrix is a strategy employed in the formation of fish fin bones and by various invertebrate phyla. This therefore appears to be a widespread strategy used by many animal phyla, including vertebrates.

1. Introduction

The vertebrate skeleton is a unique organic–inorganic tissue that forms during embryonic development and is dynamically shaped and maintained throughout the animal's life (Currey, 2002). Bones are complex structures, with a hierarchical organization encompassing a range from nanometers to centimeters (Weiner and Traub, 1992; Weiner and Wagner, 1998). At the fundamental structural level, all bones are comprised of type-I collagen fibrils reinforced by co-aligned crystalline platelets of carbonated hydroxyapatite, a calcium phosphate mineral (Landis et al., 1993; Traub et al., 1989). Various cell types are responsible for the formation as well as the maintenance of the bone integrity and function (Peck and Woods, 1988).

Bones of the vertebrate skeleton may develop *via* two distinct processes: intramembranous bone formation that proceeds through direct mineralization of a newly formed type-I collagen matrix and endochondral bone, involving the formation of a mineralized cartilaginous precursor that is later replaced by a mineralized bone matrix (Caplan, 1987; Streeter, 1949). In both modes osteoblasts orchestrate the bone formation process, initiated by the synthesis of an organic extracellular matrix – the osteoid (Caplan, 1987), mainly composed of type-I collagen, but also containing up to 10% non-collagenous proteins (Lowenstam and Weiner, 1989). Mineralization of the collagen fibrils thereafter takes place.

Blood serum is the main source of ions in the vertebrate body, and contains significant concentrations of calcium and phosphate, sufficient for the deposition of carbonated hydroxyapatite (Jahnen-Dechent, 2000; Posner et al., 1978). However, the pathways through which the ions are translocated from the serum to the site of deposition within the extracellular matrix, and the precise involvement of cellular processes in mineral deposition are not clear (Gay et al., 2000). Two principal modes have been suggested to describe mineral deposition into collagen matrices: (i) crystals are actively nucleated from solution by charged non-collagenous proteins associated to the collagen gap zones, without intervention of intracellular processes (Glimcher, 1984; Veis and Perry, 1967);

* Corresponding author. Present address: Department of Molecular Structural Biology, Max Planck Institute of Biochemistry, Am Klopferspitz 18, 82152 Martinsried, Germany. Fax: +49 89 8578 2641.
E-mail address: mahamid@biochem.mpg.de (J. Mahamid).

1047-8477/$ - see front matter © 2011 Elsevier Inc. All rights reserved.
doi:10.1016/j.jsb.2011.03.014

(ii) matrix vesicles that bud from the plasma membrane accumulate ions extracellularly by virtue of their macromolecular composition (Ali et al., 1970; Anderson et al., 2005). Both modes may be active in the same tissue. A third alternative mode has been more recently proposed based on *in vitro* and *in vivo* observations, namely that an amorphous mineral precursor is transiently formed and deposited within the gap zones inside the collagen fibril, followed by crystallization into hydroxyapatite (Mahamid et al., 2008, 2010; Olszta et al., 2007; Weiner, 2008). This strategy is widely employed by many invertebrates for the formation of their calcium carbonate mineralized tissues (Weiner et al., 2009). Deposition of amorphous precursors, rather than ion sequestration from solution, offers major advantages for packaging, transport and extracellular deposition of ions during biomineralization (Weiner et al., 2005).

We have previously shown in the continuously forming fin bony rays of Tuebingen long fin zebrafish, that mineralization of the bone collagenous matrix proceeds *via* infiltration of a nanospherulitic amorphous calcium phosphate (ACP) precursor phase (Mahamid et al., 2008, 2010). This precursor later transforms within the collagen fibrils into crystalline carbonated hydroxyapatite. The formation and packaging of the ACP particles occur within bone-lining cells, found in contact with the bone growth zones. The organization of the crystals in the collagenous matrix in the zebrafish fin bones is the same as the mineralized collagen organization in mammals (Mahamid et al., 2008), yet this system still represents a simplified vertebrate model of skeletal bone formation. To assess whether the amorphous precursor phase strategy and our observations of collagen mineralization pathways in the zebrafish model may be a general feature of bone mineralization, we undertook this study on the mineralization processes in developing bones of a mouse model.

Calvarial bones are the classic example of intramembranous bone formation. The first mineralization centers are observed as early as embryonic day 14.5 (E14.5), in the shape of bone trabeculae (Kaufman, 1994). As the bones grow, areas between trabeculae are filled in by new bone, eventually resulting in a solid plate (Aaron, 1973). In contrast to calvaria, the long bones of the limbs grow in length by endochondral calcification, but thickening is achieved by intramembranous calcification (Caplan, 1987). Mineralization starts at late pregnancy (E15–15.5) with the formation of a mineralized ring around the cartilage core at the mid-diaphysis (Kaufman, 1994), which undergoes expansion by repetitive centrifugal deposition of mineralized struts on the outer surface of the previous ring (Caplan, 1987). Previous studies on neonatal mouse calvaria presented strong indications for the possible involvement of disordered precursor phases during mineralization (Carter et al., 1997; Crane et al., 2006).

Calvaria and long bones from wild type embryonic and neonatal mice were freshly dissected, immediately high pressure frozen and imaged in their native hydrated state using cryogenic electron microscopy. By applying cryo-sample preparation methodology for high resolution cryo-electron microscopy imaging and analysis, artifacts involving ion diffusion and mineral dissolution/crystallization can be practically eliminated, while enabling observation of intact cellular and extracellular tissues. Cryo-SEM observations were made to characterize the forming bone tissue morphology and to detect the earliest mineral phase. Frozen hydrated thin sections of the tissues were visualized by cryo-TEM and subjected to selected area electron diffraction, and freeze-dried for combined characterization of TEM electron diffraction and elemental analysis on the mineral. Together, these techniques show that cells of the osteoblast-lineage concentrate calcium and phosphate ions within intracellular compartments in the form of a disordered mineral precursor phase. The mineral particles are then extruded into the extracellular collagen matrix, where they eventually crystallize.

2. Materials and methods

2.1. Animals

C57/Bl6 mice were purchased from Harlan Laboratories (Jerusalem, Israel). For osteoblast-lineage tracing experiments, Col1a1-Cre (Dacquin et al., 2002) and ROSA-YFP reporter mice (Engleka et al., 2005) were purchased from Jackson Laboratory. In all timed pregnancies, plug date was defined as E0.5. For harvesting of embryos, pregnant female mice were sacrificed by CO_2 intoxication. The gravid uterus was dissected out and suspended in a bath of cold PBS and the embryos were harvested after amnionectomy and removal of the placenta. Tail genomic DNA was used for genotyping. Calvaria and long bones were dissected immediately after the animal was sacrificed and frozen within 30 min from the time of death.

2.2. Micro-computed tomography (μ-CT)

The harvested bones were fixed overnight in 4% PFA in PBS, followed by dehydration to 70% ethanol. Samples were scanned using a microfocussed X-ray tomographic system (MICRO XCT-400, Xradia), at 40 kV and 200 μA. 1000 projection images at a total integration time of 20 ms with a linear magnification of 4× were taken. The final pixel size was 2.1 microns. Images were reconstructed using the software provided by the microCT systems and a 3D viewer (Xradia) was used to produce the 3D volume rendering.

2.3. Histology

For charecterization of the cellular tissue, bones were fixed overnight in 4% PFA/PBS and decalcified at 4 °C in 19% EDTA (pH 7.4) for 6 days. Then, tissues were dehydrated to 100% ethanol, embedded in paraffin and sectioned at 5 μm. Sections were stained using standard hematoxylin and eosin protocol. For detection of osteoblasts by immunofluorescence, sections from Col1a1-Cre, ROSA-YFP mouse line were incubated overnight at 4 °C with the primary antibody biotinilated goat anti-GFP (Abcam), diluted 1:50 in blocking solution.

Direction and timing of bone deposition was evaluated by intraperitoneal injections of calcein (2.5 mg/kg body weight, Sigma–Aldrich) at E15.5 and Alizarin complexone (7.5 mg/kg, Sigma–Aldrich) at E16.5 into pregnant females. Before use, all fluorochrome solutions were adjusted to pH values of 7.4, sterilized by filtration and warmed to 37 °C. The harvested bones were fixed overnight in 4% PFA in PBS, followed by dehydration to 100% ethanol and embedding in Epon. Sections of 4 μm were produced, and either stained with Toluidine blue for general tissue histology, or visualized using confocal microscopy (Leica DMI 4000B) for characterization of fluorochrome incorporation into the mineralized tissue.

2.4. Cryo-SEM

Fragments of about 2 mm × 2 mm were cut from freshly dissected calvaria samples. Long bones dissected from the limbs were used whole. The samples were immediately immersed in 10% Dextran (Fluka), sandwiched between two metal discs (3 mm diameter, with 0.1 or 0.2 mm cavities) and cryo-immobilized in a high pressure freezing device HPM10 (Bal-Tec). The frozen samples were mounted on a holder under liquid nitrogen and transferred to a Freeze Fracture device BAF 60 (Bal-Tec) using a Vacuum Cryo Transfer device VCT 100 (Bal-Tec). Samples were fractured at −140 °C, etched for 20 min at −105 °C under a vacuum better than 5×10^{-7} mbar and coated with 2.5 nm Pt/C by double axis rotary shadowing. Alternatively, samples were frozen within a 0.2 mm cavity disc and covered

by a flat disc. Frozen samples were transferred to a cryo-ultramicrotome (Leica) and trimmed using a 20° trimming diamond knife (Diatome) for the production of a transverse surface view of the bones. These samples were then transferred to the BAF 60 for etching and coating as described above. Samples were observed in an Ultra 55 SEM (Zeiss) using a secondary electron in-lens detector and a backscattered electron in-lens detector (operating at 5 kV; ESB grid operating at 500 eV) in the frozen-hydrated state by use of a cryo-stage at a temperature of −120 °C.

2.5. Cryo-TEM

Calvaria samples, high pressure frozen in a 0.2 mm cavity disc and covered by a flat disc, were transferred to the cryo-chamber of an ultracryomicrotome (Leica). The two discs were separated carefully, while maintaining the frozen tissue within the cavity of the metal disc. The sample was then mounted in a clamp sample holder of the cryo-chamber. The sample block was trimmed with a 20° trimming diamond knife (Diatome) and cryo-sectioned at −160 °C using a 35° diamond knife (Diatome). The 100 nm thick sections were transferred to a copper grid with a thin holey carbon support (C-flat, EMS) using an eyelash glued to a wooden stick, and then pressed with a cryo-tool (composed of two polished ceramic surfaces) to ensure good attachment to the grid. The grids were transferred to a Gatan cryo-specimen holder using a Gatan cryo-transfer apparatus and examined in an FEI (Philips) T120-Technai TEM operating at 120 kV, at a temperature of −180 °C, under low dose conditions. The electron diffraction patterns were recorded using a selected area aperture allowing observation of a circular area with diameter of 200 nm.

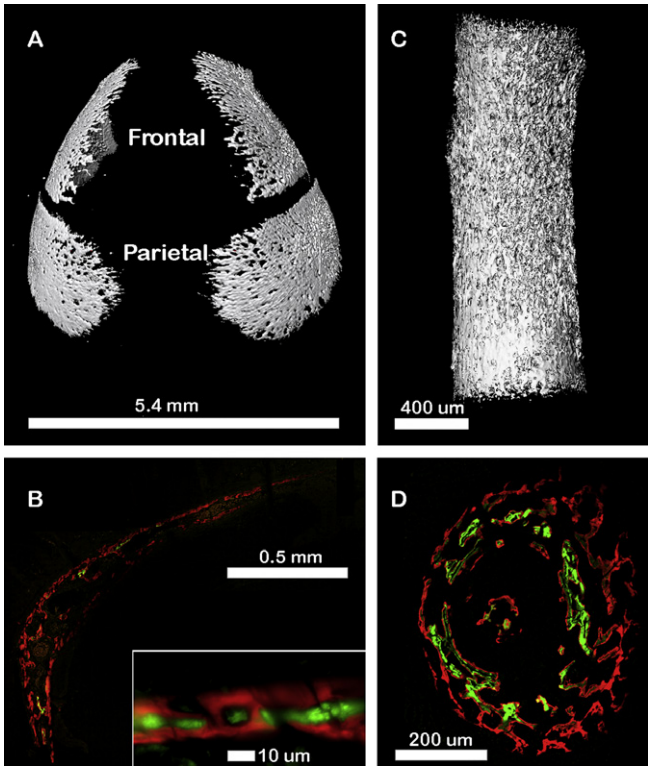

Fig. 1. A, C: μ-CT image of E17 calvaria showing the mineralized portions of the frontal and parietal paired bones undergoing intramembranous calcification (A) and an image of E18 Femur undergoing endochondral and periosteal calcification (C). **B, D:** Sequential calcein (E15.5, Green) and alizarin (E16.5, Red) incorporation into the mineralizing bones during late pregnancy in calvaria harvested at P1 (B) and femur harvested at E17.5 (D). **B:** Calvarial bone shown in coronal plane grows rapidly, with massive formation of new bone after E16.5 (red stain). Each trabecula grows in thickness (inset). **D:** Cross-section of the femur taken from the mid shaft shows that the bone collar (green stain) is the first mineralized structure. The outer mineralized bone rings form at later stages (red stain).

2.6. TEM, selected area electron diffraction and energy dispersive spectroscopy (EDS)

Vitrified frozen sections were freeze dried under high vacuum in the BAF 60 and brought to room temperature. Observations and measurements were performed using a Philips CM120 Super Twin TEM (120 kV, tungsten/LaB6). EDS spectra were collected from areas of 200 nm in diameter, and calcium/phosphate ratios were calculated as the calibrated ratio between the atomic percentages of the two elements. The electron diffraction patterns were also recorded using a selected area aperture with 200 nm diameter. Calibration of diffraction patterns was done relative to diffraction patterns from a gold standard obtained at the same working distance.

3. Results

We examined the process of bone formation in two developing bone types: calvarial parietal bones of mice during the period of embryonic day 17 (E17) to postnatal day 2 (P2), and long bones (femur and humerus) during the period of E16 to E18. μ-CT was used to characterize the general morphology of the mineralized tissue at the micrometer scale. E17 calvaria parietal bones appear as thin plates composed of a network of trabeculae (Fig. 1A) that are a few millimeter in length and width and approx. 100 μm in thickness. Sequential calcein and alizarin injections during late pregnancy enabled identification of the bone growth directions and the extent of mineral deposition. Calvarial bones grow rapidly, with formation of new mineralized tissue both on the top and bottom surfaces (in the dorso-ventral direction) of each trabecula (Fig. 1B and inset). Mineralized parts of E18 femur examined with μ-CT are less than 2 mm long, and about 500 μm in diameter (Fig. 1C). In cross-section, the innermost bone collar is the first to form after injection of calcein, as indicated by sequential fluorochrome incorporation. The bone collar is highly mineralized (Figs. 1D and 2A, B). The outer mineralized bone rings form at later stages and also display lower mineral contents (Figs. 1D and 2A, B).

In agreement with the growth directions observed in the developing bones, histological calvaria sections stained with hematoxylin and eosin show that the forming bone surfaces are lined with an almost continuous monolayer of cuboidal cells, reminiscent of osteoblasts (Supplementary Fig. 1A, B) (Aaron, 1973). To unambiguously clarify the identity of the bone-lining cells, we performed osteoblast-lineage tracing experiments utilizing Col1a1-Cre, ROSA-YFP mice. Numerous cells at the bone surface produce specific labeling using an anti-GFP antibody, confirming their identity as differentiated osteoblasts (Supplementary Fig. 1C). Osteocytes residing within the mineralized bone also produce fluorescent labeling.

Utilizing cryo-SEM for high resolution characterization of the mineralization stages, we were able to identify loci of new bone formation in the long bones based on whole bone morphology (Fig. 2A, B). The innermost surfaces – the bone collar – are highly mineralized, as shown by the extracellular matrix texture and the strong signal in backscattered electrons imaging. Trabeculae were found on the outer surfaces of the bone that were mostly organic, i.e. composed of densely packed collagen fibrils, but also contained non-continuous sub-micrometer mineral islands. Lining the forming trabeculae are well preserved osteoblasts facing a non-mineralized fibrillar collagen matrix- the osteoid (Fig. 2C). The extracellular matrix in each trabecula gradually becomes more mineralized by the

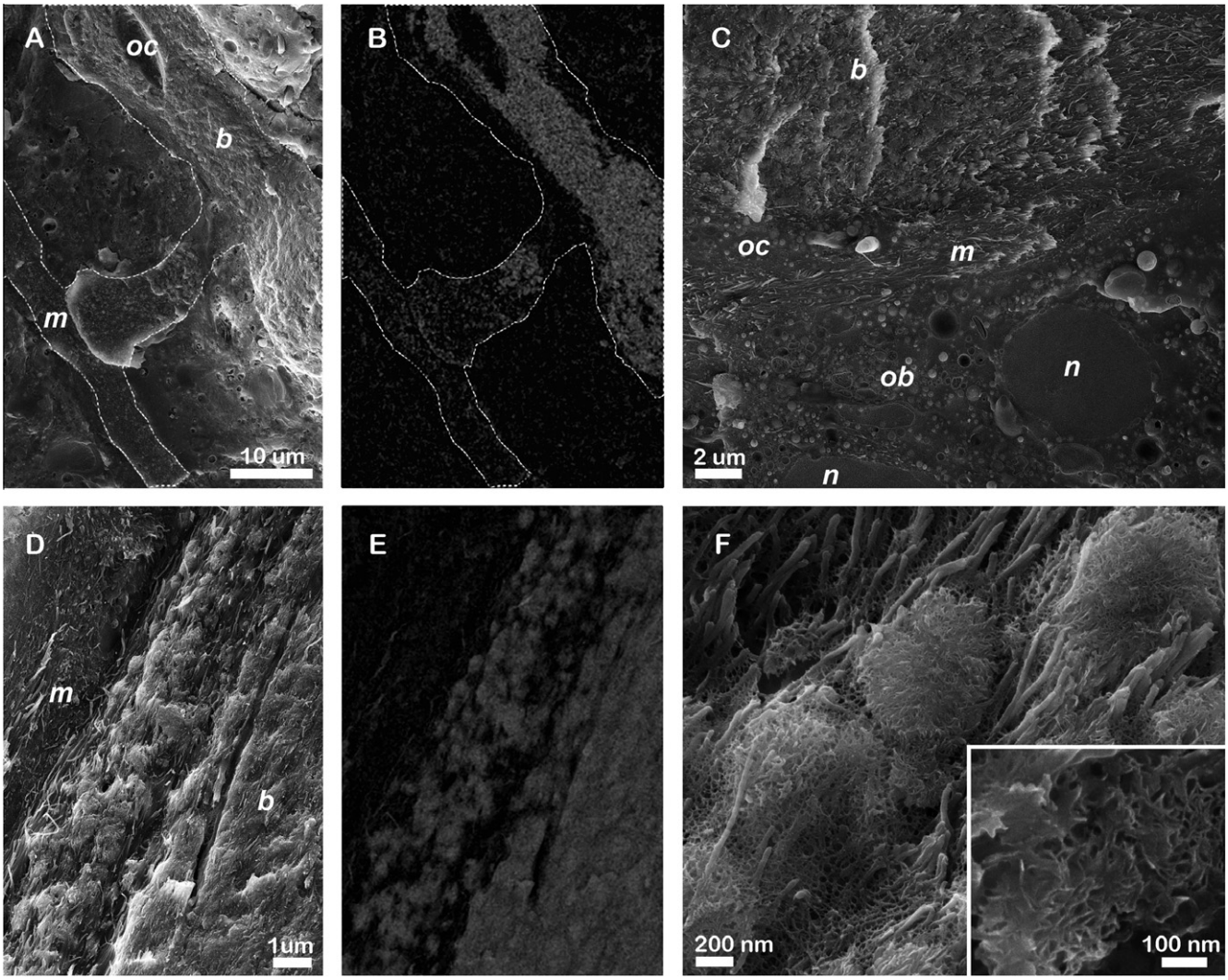

Fig. 2. Cryo-SEM micrographs of freeze fractured embryonic mouse long bones. **A:** E16 femur showing two consecutive connected bone trabeculae (delineated). The inner trabecula (b) is heavily mineralized, while mineralization in the second (m), outer trabecula is only beginning. **B:** Corresponding backscattered electrons image. **C:** Osteoblasts line the bone surface of a mineralizing trabecula in E17.5 long bone. **D, E:** Progressive mineralization of a trabecula in E18 humerus (increased mineralization from left to right). **E:** Corresponding backscattered electrons image. **F:** Extracellular mineralizing matrix in E16 femur showing the nodule organization of the newly-deposited mineral interspersed in between collagen fibrils. Inset: Mineral shows a flake-like morphology. *m – non-mineralized matrix; b – bone; ob – osteoblast; oc – osteocyte; n – nucleus.*

addition of mineral packets (Fig. 2D, E). At higher magnifications, the extracellular mineral was often observed to be arranged in the form of nodules, a few hundred nanometers in diameter, dispersed between the collagen fibrils (Fig. 2F). The single mineral particles are very thin, curved, flat platelets (Fig. 2F: Inset). We inferred that these are the newly-deposited mineral species.

Identification of discrete bone formation loci in the calvarial bones was not as clear as in the various long bones. Mineralized extracellular structures of two types were observed in calvaria. The first, displaying an appearance similar to the newly formed trabeculae of the long bones, consists of mineral nodules interspersed within a dense collagenous matrix (Fig. 3A, B). The second consists of loosely packed single fibrils undergoing mineralization (Fig. 3C, D), such that one part of the fibril is impregnated with mineral while at the other end, the fibril is still un-mineralized.

Cryo-SEM imaging of cryo-sectioned flat block faces from the developing bone samples enables morphological identification of the different cell types involved in bone formation: from pre-osteoblasts, through cuboidal osteoblasts lining the forming bone surfaces and osteocytes becoming embedded within the mineralizing extracellular matrix (Supplementary Fig. 2). Osteoblasts and osteocyte morphologies observed by cryo-SEM were consistent with the locations at which fluorescence labeling was produced in the osteoblast-lineage tracing experiments (Supplementary Fig. 1C). Examination of the cells lining the forming bone surface revealed the presence of intracellular mineral (Figs. 3 and 4, arrowheads). The intracellular mineral is always contained within vesicles of approximately 1 μm diameter, is typically aggregated into round globules mostly found in contact with the vesicle membrane, and is often interconnected by fibrillar structures (Figs. 3 and 4). The mineral globules are on average 80 nm in diameter, and these in turn are composed of smaller (up to 10 nm) spheres (Fig. 4B–E and insets therein). The nano-spherical mineral subunits are reminiscent of the intracellular and extracellular ACP nano-spheres dominating the newly-formed bones of the zebrafish fin (Mahamid et al., 2008, 2010). The presence of intracellular mineral vesicles was observed in pre-osteoblasts, osteoblasts and osteocytes (Supplementary Fig. 2C–H). Each cell observed contained numerous mineral-bearing vesicles (see for example: Fig. 3E, F). In samples of long bones, mineral-bearing vesicles were observed with the

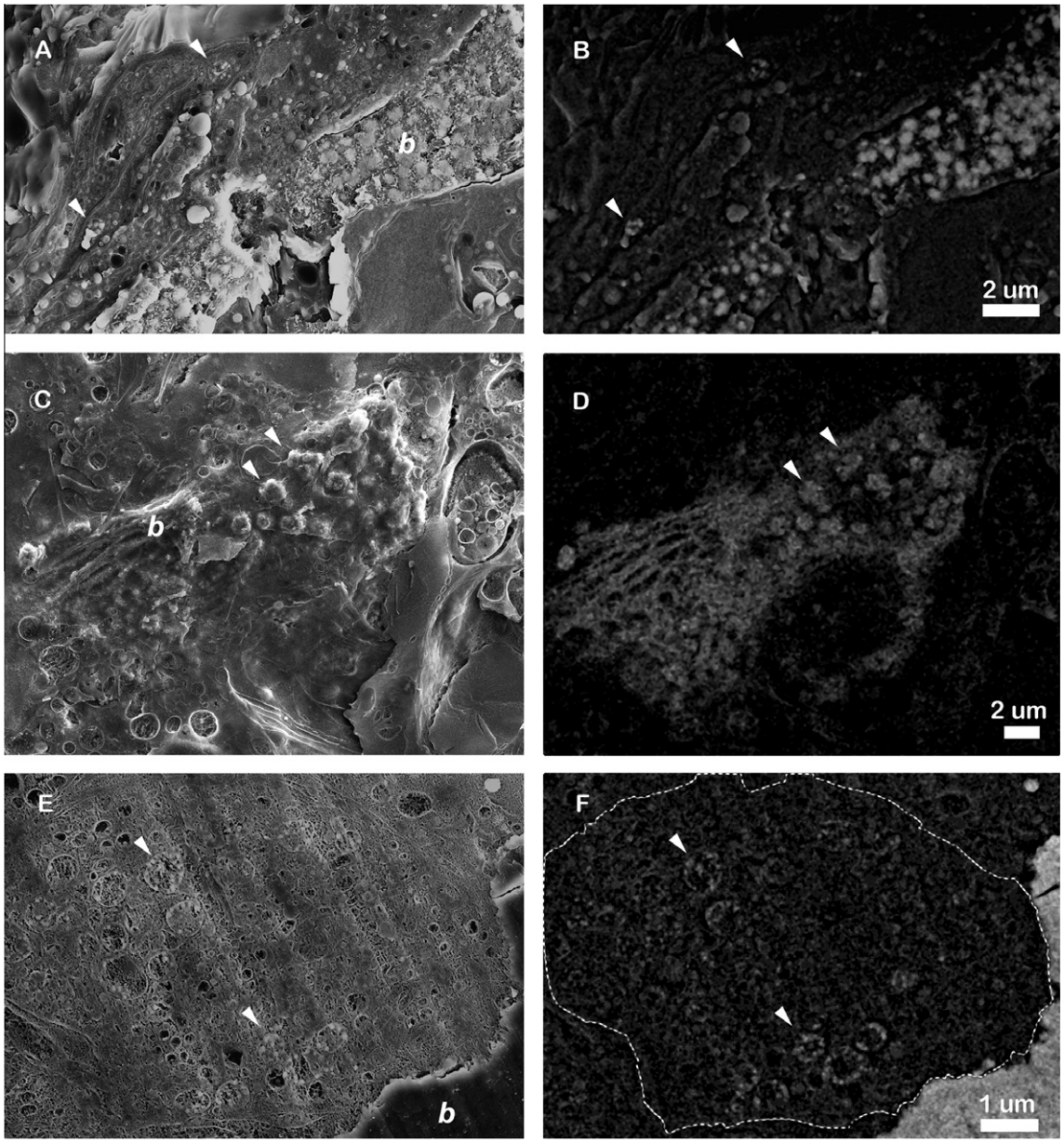

Fig. 3. Cryo-SEM micrographs of freeze fractured (A–D) and cryo-sectioned (E, F) embryonic mouse neonatal calvarial bones. Right panel are the corresponding backscattered electrons images. **A, B:** E17 calvaria showing an extracellular mineralized matrix (b) and intracellular mineral vesicles (arrowheads) in a cell process adjacent to the bone matrix. The bone matrix is impregnated with mineral nodules. **C, D:** E17 calvaria showing an extracellular loose mineralized matrix (b) and intracellular mineral vesicles (arrowheads). **E, F:** P1 calvaria showing a dense extracellular mineralized matrix (b) and numerous mineral-containing vesicles (arrowheads) in a cell lining the bone. Higher magnification of the same vesicles is shown in Fig. 4. B, C. The cell's circumference is clearly delineated by a membrane (highlighted in F). Lineation observed in the cryo-sectioned block face is a sectioning artifact.

same characteristic as in calvaria (Fig. 4B, D), but their occurrence was more sporadic.

Frozen thin sections obtained from equivalent E17 and P1 calvarial tissue preparations, observed in cryo-TEM, showed that indeed the bone lining cells often contain electron dense, membrane-bound mineral globules (Fig. 5A: arrowhead, B). Selected area electron diffraction of the vesicles resulted only in an amorphous diffuse scatter (Fig. 5G); whereas the adjacent fully mineralized extracellular matrices (Fig. 5A (b)) gave a clear crystalline hydroxyapatite diffraction pattern (Fig. 5F). Extracellular matrix mineral found at the interface between the mineralized and non-mineralized matrix displayed a thin curved appearance (Fig. 5E). Surprisingly, the mineral produced a diffuse scattering diffraction pattern consisting of rings around *d*-spacings expected for the strong (0 0 2), (2 1 1), (1 1 2) and (3 0 0) reflections of crystalline hydroxyapatite. This diffraction pattern is indicative of the presence of short or medium range order (Fig. 5H).

In order to further characterize the mineral phases observed in the cryo-preparations, we subjected cryo-sections to freeze-drying to enable TEM analysis at room temperature. The freeze-dried sections were not completely intact. However areas of interest were structurally stable enough for imaging and spectroscopic measurements (Fig. 5C and Supplementary Fig. 3). Selected area electron diffraction and elemental analysis by EDS were taken from the same positions in bone mineralized matrix, in intracellular mineral deposits and in cellular tissue for background evaluation. Electron

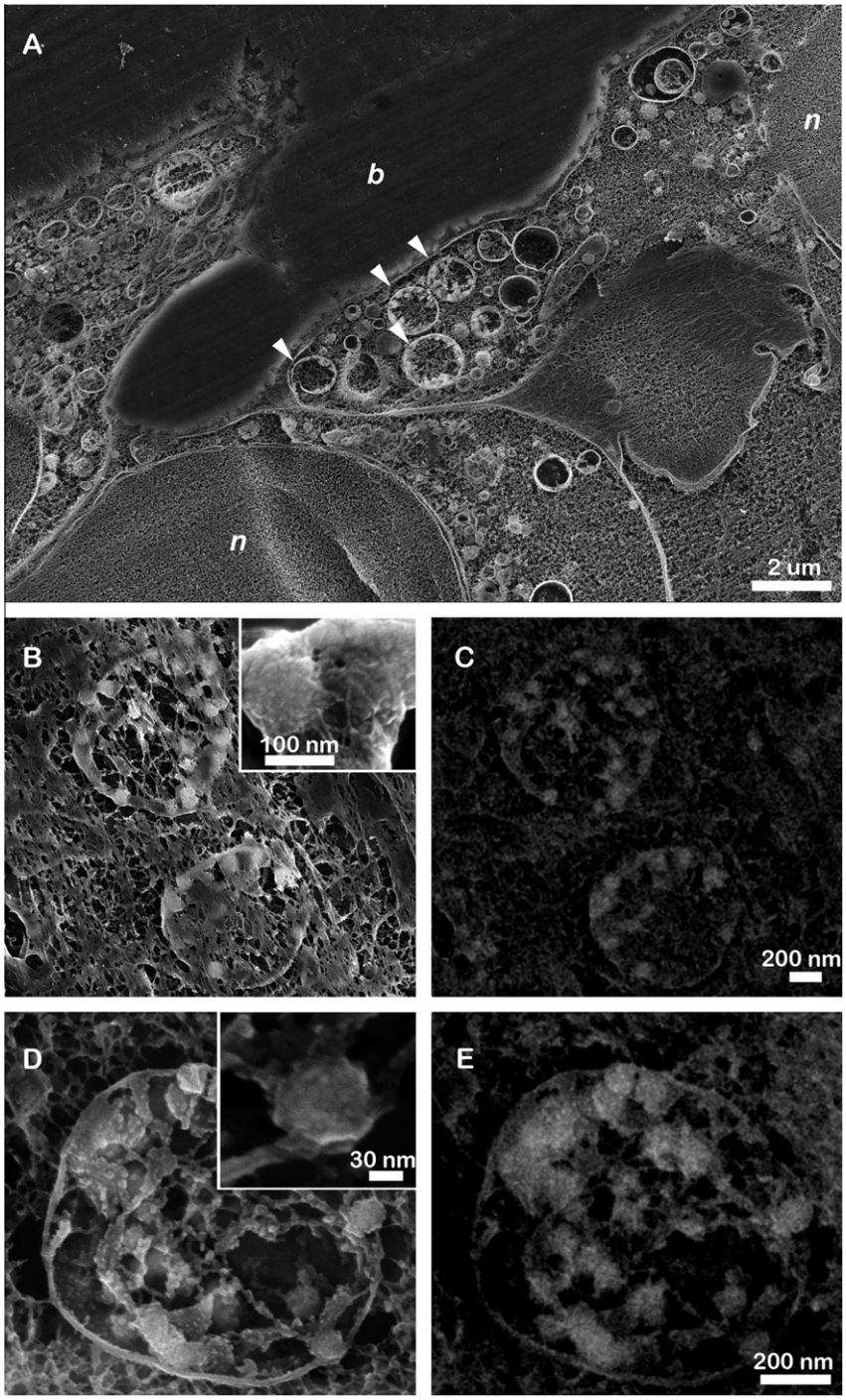

Fig. 4. Cryo-SEM micrographs of cryo-sectioned neonatal calvaria (A–C) and freeze fractured embryonic long bone (D, E). C and E are backscattered electrons images corresponding to B and D. **A:** Cells juxtaposed to a mineralizing bone trabeculae (b) with multiple intracellular mineral-containing vesicles (arrowheads). Nuclei (n) are clearly delineated by double membranes. **B, C**: Two intracellular mineral-containing vesicles in a cell process lining a mineralizing bone matrix. Inset: higher magnification of mineral globules composed of smaller nano-spheres. The micrographs are higher magnification from Fig. 3. E F. **D, E:** E18 humerus showing an intracellular mineral-containing vesicle. Inset: higher magnification of a mineral globule. The mineral globules are often membrane-bound.

diffraction of the intracellular mineral consistently produced a diffuse amorphous scatter, even after drying, and retained the appearance of nano-spherical amorphous mineral (Fig. 5D and Supplementary Fig. 3). The mineralized matrix of the bone trabeculae produced characteristic apatite diffraction patterns. Average values for calcium/phosphate ratios calculated from the measured atomic percentages were 1.58 ± 0.16 for the mineralized extracellular matrix; 0.75 ± 0.22 for the intracellular mineral-containing vesicles and 0.19 ± 0.16 for the background in the cellular tissue. The values obtained for the extracellular mineral, although lower than the expected 1.67 ratio for stoichiometric hydroxyapatite (Christoffersen et al., 1989), are within the range characteristic of mature bone mineral (Kuhn et al., 2008). Surprisingly, the value obtained for the intracellular vesicle-bound mineral, 0.75 ± 0.22,

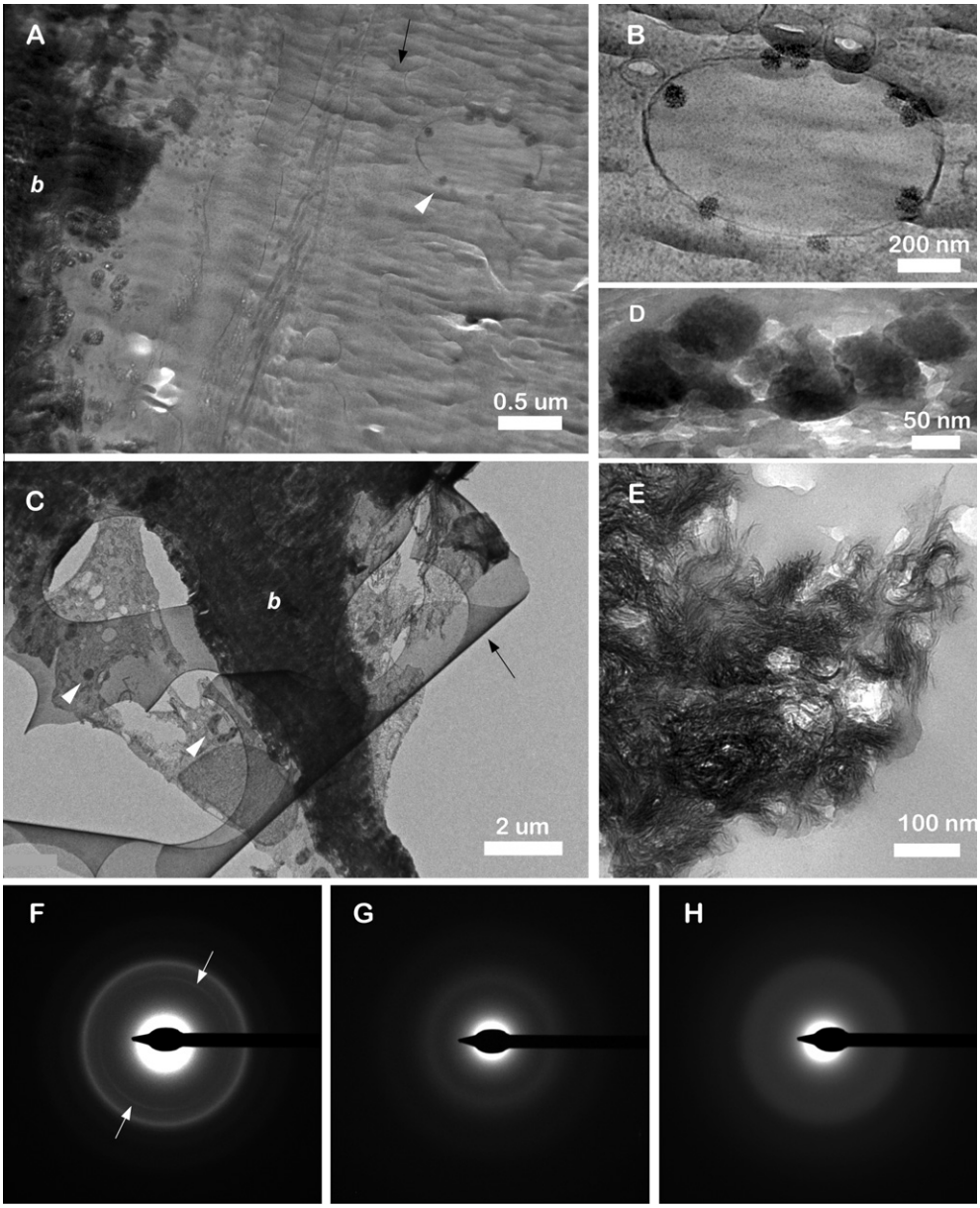

Fig. 5. TEM micrographs of cryo-sections of mouse calvarial bones. **A:** Cryo-TEM of a vitrified thin section from P1 mouse calvaria showing an extracellular mineralized matrix (b) and an intracellular mineral vesicle (arrowhead) in a cell adjacent to the mineralizing bone matrix. Black arrow points to cryo-sectioning linear artifacts. **B:** Higher magnification of the mineral-containing vesicle in A, showing a number of high electron density, membrane-bound globules. **C–E:** TEM of a freeze-dried cryo-section from E17 mouse calvaria. **C:** Extracellular mineralized matrix (b) and numerous intracellular mineral vesicles (arrowheads) in a cell adjacent to the bone matrix. The cell nucleus is clearly visible. Black arrow points to the holey-carbon film support. **D:** Higher magnification of part of a mineral-containing vesicle, showing a number of high electron density mineral particles, composed of smaller spheres. **E:** Peripheral newly-deposited extracellular mineral, with highly curved morphologies. **F:** Selected area electron diffraction of mineral, corresponding to the area marked by (b) in A. Arrows point to the (0 0 2) reflections of hydroxyapatite. **G:** Selected area electron diffraction of intracellular mineral vesicle in A and B. **H:** Selected area electron diffraction of peripheral extracellular mineral shown in E.

is far from the expected value for synthetic amorphous calcium phosphate (namely around 1.5) (Christoffersen et al., 1989).

4. Discussion

Here we show *in vivo* in a mammalian mouse model that prior to mineralization, cells lining the forming bones, including pre-osteoblasts, osteoblasts and osteocytes, concentrate ions intracellularly and produce a membrane-bound disordered calcium-phosphate phase. The mineral is found in the form of 80 nm granules, which are in turn composed of smaller spherical subunits. We suggest that the mineral-containing vesicles are directly involved in initiating extracellular mineralization and that the disordered calcium-phosphate is a precursor of carbonated hydroxyapatite.

Individual osteoblasts present on surfaces of bone where active bone formation takes place are known to tightly adhere to each other and form a continuous cell layer (Aaron, 1973; Caplan, 1987; Gay et al., 2000). This layer has long been suggested to limit direct access of ions from the body fluids to the mineralizing bone surface, and thus the mineral ions must pass through the bone-lining cells (Gay et al., 2000). Our observations clearly demonstrate an active role of the osteoblast-lineage derived cells in sequestering ions and creating intracellular 'reservoirs' of the mineral precursor.

These findings are in agreement with previous electron microscopy studies on osteoblasts, both in culture (Bordat et al., 1998, 2004; Rohde and Mayer, 2007) and from frozen tissue preparations (Carter et al., 1997; Gay and Schraer, 1975), showing intracellular compartments containing mineral deposits. Using osmium vapor staining, Gay and Schraer (1975) concluded that the mineral containing compartments are mitochondria, reinforcing previous reports of 'mitochondrial mineralization' (reviewed in (Lehninger, 1970)). Our observations of the mineral-containing vesicles do not show resemblance to the typical appearance of mitochondria, which are easily identified in cryo-SEM (Supplementary Fig. 4).

We suggest that osteoblasts directly secrete the precursor mineral into the extracellular mineralization site. We were not however able to identify the process of translocation of the intracellular mineral into the extracellular mineralizing matrix. In a study on osteoblast cell culture, Rohde and Mayer (2007) showed that intracellular mineral may be translocated to the extracellular environment directly by exocytosis.

Non-crystalline calcium phosphates are highly metastable mineral phases in water and unless stabilized by organic or inorganic additives or sealed from the surrounding solution, they quickly convert into the thermodynamically more stable carbonated hydroxyapatite crystalline phase (Posner et al., 1978). Indeed, in the extracellular matrix, inhibition over nucleation is somehow lost and crystallization occurs, giving rise to a mature mineralized bone matrix.

The amorphous mineral within the intracellular vesicles contains considerably less calcium than expected for an ACP phase. This suggests that the intracellular vesicles serve as a confined space in which relatively high concentrations of phosphate entities are formed. These could in part be in the form of phospholipids that compose the vesicle membrane, which were shown *in vitro* to complex calcium and inhibit crystallization of the forming mineral (Wuthier and Eanes, 1975). Alternatively, the high phosphate concentration may be accounted for by the presence of other organic phosphates or polyphosphate. Polyphosphates form strong complexes with divalent cations such as calcium, and can lead to a high local accumulation of total phosphate and calcium that exceeds the supersaturation limit of apatite without triggering the spontaneous precipitation of apatite crystals (Omelon and Grynpas, 2008). Such complexes, exhibiting Ca/P ratios of approximately 0.5, were recently suggested to be present at the sites of new bone formation (Omelon et al., 2009).

We previously reported that amorphous calcium phosphate is present in the forming fin bones of zebrafish, where it functions as a precursor for the mature crystalline mineral (Mahamid et al., 2008, 2010). Following recent findings from studies performed *in vitro* it appears that the amorphous nature assists infiltration of the mineral into the confined mineralization spaces within the collagen fibrils, where it eventually crystallizes (Nudelman et al., 2010; Olszta et al., 2007). Here we confirm that an amorphous mineral precursor phase occurs in mammalian bone and thus contributes to the mechanistic understanding of the involvement of osteoblasts in bone mineralization.

There are several differences in the mineralization processes between the adult zebrafish fin bones and the developing mouse bones. Intracellular mineral vesicles observed within bone-lining cells were completely filled with a dense granulated mineral in zebrafish, but the mineral does not appear to be organized into 80 nm individual granules within a vesicle as in the mouse bones. Additionally, we observed a curved flake-like mineral form in the extracellular matrix of the developing mouse bones, which did not produce a crystalline diffraction pattern. The fact that the mineral particles do not have spherical shapes, but are rather flat and curved, is reminiscent of the ACP2 phase described by Christoffersen et al. (1989), suggesting that the transformation of the intracellular phosphate-rich amorphous phase into the mature crystalline phase may involve additional intermediates. Interestingly, also in calcium carbonate-based mineralization two distinct amorphous phases were observed, representing progressive stages of the amorphous precursor transformation toward the final crystalline phase (Politi et al., 2006, 2008). The morphological differences between mineralization in the two animal models may be a consequence of different phase transformation kinetics possibly due to the differences in body temperature (ambient water temperature vs. 37 °C). Alternatively, the differences may be related to different regulatory pathways employed during mature bone growth versus *de novo* embryonic bone formation.

Deposition of pre-packaged particles of a disordered precursor phases is advantageous for the biological system, insofar as this mechanism facilitates transport of material into the newly formed matrix and avoids elimination of large amounts of water. Additionally, the mineral is provided in a form that can penetrate into the interior of the collagen fibrils, where it subsequently crystallizes. On the other hand, the finding of intracellular amorphous mineral deposits only shifts the fundamental questions of how the ions are concentrated, transiently stabilized as an amorphous phase and packaged, one step backward – to the intracellular components and subcellular compartments, the identity and the function of which still need to be clarified.

5. Conclusions

In this study we extend and expand upon our understanding of fish fin bone mineralization mechanisms to mineralization processes in forming mouse bones. The latter is widely accepted as a leading mammalian model of bone formation. Using cryo-SEM and cryo-TEM we found that *in vivo* bone-lining cells concentrate a non-crystalline calcium phosphate phase within intracellular vesicles that has a surprisingly low Ca/P ratio. These observations highlight the role of the osteoblasts as being directly responsible for the deposition of the first mineral phase in the broader context of regulating the whole bone formation process.

Acknowledgments

We thank Dr. Vlad Brumfeld for his assistance with fluorescence and μ-CT imaging. The electron microscopy studies were conducted at the Irving and Cherna Moskowitz Center for Nano and Bio-Nano Imaging, Weizmann Institute of Science. L.A. is the incumbent of the Dorothy and Patrick Gorman Professorial Chair of Biological Ultrastructure, and S.W. is the incumbent of the Dr. Trude Burchardt Professorial Chair of Structural Biology. J.M. was supported by the Israeli Council for Higher Education. This work was supported by the Kimmelman Center for Biomolecular Structure and Assembly, Weizmann Institute.

Appendix A. Supplementary data

Supplementary data associated with this article can be found, in the online version, at doi:10.1016/j.jsb.2011.03.014.

References

Aaron, J.E., 1973. Osteocyte types in the developing mouse calvarium. Calcif. Tissue Res. 12, 259–279.

Ali, S.Y., Sajdera, S.W., Anderson, H.C., 1970. Isolation and characterization of calcifying matrix vesicles from epiphyseal cartilage. Proc. Natl Acad. Sci. USA 67, 1513–1520.

Anderson, H.C., Garimella, R., Tague, S.E., 2005. The role of matrix vesicles in growth plate development and biomineralization. Front. Biosci. 10, 822–837.

Bordat, C., Bouet, O., Cournot, G., 1998. Calcium distribution in high-pressure frozen bone cells by electron energy loss spectroscopy and electron spectroscopic imaging. Histochem. Cell Biol. 109, 167–174.

Bordat, C., Guerquin-Kern, J., Lieberherr, M., Cournot, G., 2004. Direct visualization of intracellular calcium in rat osteoblasts by energy-filtering transmission electron microscopy. Histochem. Cell Biol. 121, 131–138.
Caplan, A.I., 1987. Bone development and repair. BioEssays 6, 171–175.
Carter, D.H., Hatton, P.V., Aaron, J.E., 1997. The ultrastructure of slam-frozen bone mineral. Histochem. J. 29, 783–793.
Christoffersen, J., Christoffersen, M.R., Kibalczyc, W., Andersen, F.A., 1989. A contribution to the understanding of the formation of calcium phosphates. J. Cryst. Growth 94, 767–777.
Crane, N.J., Popescu, V., Morris, M.D., Steenhuis, P., Ignelzi, M.A., 2006. Raman spectroscopic evidence for octacalcium phosphate and other transient mineral species deposited during intramembranous mineralization. Bone 39, 434–442.
Currey, J.D., 2002. Bones: Structure and Mechanics. Princeton University Press, Oxford, UK.
Dacquin, R., Starbuck, M., Schinke, T., Karsenty, G., 2002. Mouse alpha1(I)-collagen promoter is the best known promoter to drive efficient Cre recombinase expression in osteoblast. Dev. Dyn. 224, 245–251.
Engleka, K.A., Gitler, A.D., Zhang, M., Zhou, D.D., High, F.A., Epstein, J.A., 2005. Insertion of Cre into the Pax3 locus creates a new allele of Splotch and identifies unexpected Pax3 derivatives. Dev. Biol. 280, 396–406.
Gay, C.V., Schraer, H., 1975. Frozen thin-sections of rapidly forming bone: Bone cell ultrastructure. Calcif. Tissue Res. 19, 39–49.
Gay, C.V., Gilman, V.R., Sugiyama, T., 2000. Perspectives on osteoblast and osteoclast function. Poult. Sci. 79, 1005–1008.
Glimcher, M.J., 1984. Recent studies of the mineral phase in bone and its possible linkage to the organic matrix by protein-bound phosphate bonds. Philos. Trans. R. Soc. B-Biol. Sci. 304, 479–508.
Jahnen-Dechent, W., 2000. Lot's wifes problem revisited: How we prevent pathological calcification. In: Bäuerlein, E. (Ed.), Biomineralization: Progress in Biology, Molecular Biology and Application. Wiley-VCH, Weinheim, pp. 243–282.
Kaufman, M.H., 1994. The Atlas of Mouse Development. Elsevier Academic Press, London.
Kuhn, L.T., Grynpas, M.D., Rey, C.C., Wu, Y., Ackerman, J.L., Glimcher, M.J., 2008. A comparison of the physical and chemical differences between cancellous and cortical bovine bone mineral at two ages. Calcif. Tissue Int. 83, 146–154.
Landis, W.J., Song, M.J., McEwen, L.A.L., McEwen, B.F., 1993. Mineral and organic matrix interaction in normally calcifying tissue visualized in three dimensions by high voltage electron microscopic tomography and graphic image reconstruction. J. Struct. Biol. 110, 39–54.
Lehninger, A.L., 1970. Mitochondria and calcium transport. Biochem. J. 119, 129–138.
Lowenstam, H.A., Weiner, S., 1989. On Biomineralization. Oxford University Press, New York.
Mahamid, J., Sharir, A., Addadi, L., Weiner, S., 2008. Amorphous calcium phosphate is a major component of the forming fin bones of zebrafish: Indications for an amorphous precursor phase. Proc. Natl Acad. Sci. USA 105, 12748–12753.
Mahamid, J., Aichmayer, B., Shimoni, E., Ziblat, R., Li, C., Siegel, S., Paris, O., Fratzl, P., Weiner, S., Addadi, L., 2010. Mapping amorphous calcium phosphate transformation into crystalline mineral from the cell to the bone in zebrafish fin rays. Proc. Natl Acad. Sci. USA 107, 6316–6321.
Nudelman, F., Pirterse, K., George, A., Bomans, P.H.H., Friedrich, H., Brylka, L.J., Hilbers, P.A.J., de With, G., Sommerdijk, N.A.J.M., 2010. The role of collagen in bone apatite formation in the presence of hydroxyapatite nucleation inhibitors. Nat. Mater. 9, 1004–1009.
Olszta, M.J., Cheng, X.G., Jee, S.S., Kumar, R., Kim, Y.Y., Kaufman, M.J., Douglas, E.P., Gower, L.B., 2007. Bone structure and formation: A new perspective. Mater. Sci. Eng. R 58, 77–116.
Omelon, S., Georgiou, J., Henneman, Z.J., Wise, L.M., Sukhu, B., Hunt, T., Wynnyckyj, C., Holmyard, D., Bielecki, R., Grynpas, M.D., 2009. Control of vertebrate skeletal mineralization by polyphosphates. PLoS ONE 4, e5634.
Omelon, S.J., Grynpas, M.D., 2008. Relationships between polyphosphate chemistry, biochemistry and apatite biomineralization. Chem. Rev. 108, 4694–4715.
Peck, W.A., Woods, W.L., 1988. The cells of bone. In: Riggs, L., Melton, L.J. (Eds.), Osteoporosis: Etiology, Diagnosis and Management. Raven Press, New York (pp. 1–44).
Politi, Y., Levi-Kalisman, Y., Raz, S., Wilt, F., Addadi, L., Weiner, S., Sagi, I., 2006. Strucutural characterization of the transient calcium carbonate amorphous precursor phase in sea urchin embryos. Adv. Funct. Mater. 16, 1289–1298.
Politi, Y., Metzler, R.A., Abrecht, M., Gilbert, B., Wilt, F.H., Sagi, I., Addadi, L., Weiner, S., Gilbert, P.U.P.A. , 2008. Transformation mechanism of amorphous calcium carbonate into calcite in the sea urchin larval spicule. Proc. Natl Acad. Sci. USA 105, 20045.
Posner, A.S., Betts, F., Blumenthal, N.C., 1978. Properties of nucleating systems. Me. Bone Dis. & Rel. Res. 1, 179–183.
Rohde, M., Mayer, H., 2007. Exocytotic process as a novel model for mineralization by osteoblasts in vitro and in vivo determined by electron microscopic analysis. Calcif. Tissue Int. 80, 323–336.
Streeter, G.L., 1949. Developmental horizons in human embryos; a review of the histogenesis of cartilage and bone. Contrib. Embryol. 33, 149–168.
Traub, W., Arad, T., Weiner, S., 1989. Three dimensional ordered distribution of crystals in turkey tendon collagen fibers. Proc. Natl Acad. Sci. USA 86, 9822–9826.
Veis, A., Perry, A., 1967. The phosphoprotein of the dentin matrix. Biochemistry 6, 2409–2416.
Weiner, S., 2008. Biomineralization: A structural perspective. J. Struct. Biol. 163, 229–234.
Weiner, S., Traub, W., 1992. Bone structure: From angstroms to microns. FASEB J. 6, 879–885.
Weiner, S., Wagner, H.D., 1998. The material bone: Structure–mechanical function relations. Annu. Rev. Mater. Sci. 28, 271–298.
Weiner, S., Sagi, I., Addadi, L., 2005. Choosing the path less travelled. Science 309, 1027–1028.
Weiner, S., Mahamid, J., Politi, Y., Ma, Y., Addadi, L., 2009. Overview of the amorphous precursor phase strategy in biomineralization. Front. Mater. Sci., China 3, 104–108.
Wuthier, R.E., Eanes, E.D., 1975. Effect of phospholipids on the transformation of amorphous calcium phosphate to hydroxyapatite in vitro. Calcif. Tissue Res. 19, 197–210.